communications biology

Article

https://doi.org/10.1038/s42003-024-07112-6

Development of a two component system based biosensor with high sensitivity for the detection of copper ions

Check for updates

Yu Fu[1,2,3], Jiajia Li[1], Jin Wang[2,3,4], Erkang Wang[2,3] & Xiaona Fang[1] ✉

Recent advancements in bacterial two-component systems (TCS) have spurred research into TCS-based biosensors, notably for their signal amplification and broad input responsiveness. The CusRS system in *Escherichia coli (E. coli)*, comprising *cusS* and *cusR* genes, is a copper-sensing module in *E. coli*. However, due to insufficient sensing performance, CusRS-based biosensors often cannot meet practical requirements. To address this issue, we made improvements and innovation from several aspects. CusR and CusS expression were adjusted to enhance the Cu(II) biosensor's performance. A copy-number inducible plasmid was used for signal amplification, while removing copper detox genes *cueO* and *cusCFBA* improved sensitivity and lowered detection limits. Ultimately, in the optimized biosensor of Cu26, the fold-change (I/I_0) increased from 1.5-fold to 18-fold at 1 μM, rising to 100-fold after optimizing the cell culture procedure. The biosensor's high fluorescence enabled rapid, instrument-free detection and an improved analysis strategy reduced the detection limit to 0.01 μM, surpassing traditional methods.

Copper ions, found in nature and human activities, have both positive and negative effects on human health and the environment[1,2]. Excessive intake can lead to health issues[3], like gastrointestinal discomfort, vomiting. In severe cases, it can cause damage to organs such as the liver, gallbladder, and kidneys, as well as irritation to the eyes and skin. In addition to its effects on human health, industrial discharge can harm ecosystems and water sources[4,5]. Consequently, the detection of copper ion content is crucial for human health and environmental quality[1,6].

With the rise of recombinant DNA technology, whole cell biosensors have experienced significant advancements[7,8]. Microbial sensors are user-friendly, cost-effective, and exhibit high reproducibility. They can assess analyte bioavailability to living systems in a physiologically relevant manner, with a broad detection range and high efficiency[8–11]. *Escherichia coli (E. coli)* exhibits resistance to copper ion exposure due to two key systems that regulate copper ion levels. The cue system, with CueR as a crucial factor, activates the promoter of P_{copA} in response to copper ions, regulating the expression of *copA* and *cueO* genes. CopA facilitates copper ion efflux, while CueO catalyzes the oxidation of Cu(I) to Cu(II) in the periplasmic space[12,13]. This system has been identified as the predominant mechanism for copper resistance in *E. coli* under both aerobic and anaerobic conditions[14–16]. Another system involved in controlling copper levels in *E. coli* is CusRS two-component system, which consists of *cusR* and *cusS* genes. It plays a crucial role in maintaining the balance of Cu(I) in the periplasm. CusS, a histidine kinase located in the inner membrane, is responsible for senseing Cu(I) in the periplasmic space. Upon binding to Cu(I), CusS undergoes a conformational change that activates its kinase domain. This activation results in autophosphorylation and subsequently activates CusR through the transfer of a phosphate group[17]. The phosphorylated CusR activates the expression of the *cusRS* genes through the P_{cusR} promoters, as well as the *cusCFBA* genes through P_{cusC}, which work together to expel Cu(I) from the cell, maintaining low copper ion levels[18,19].

Microbial-based copper sensors have been extensively studied, but most rely on the CueR system, which lacks sensitivity. This deficiency leads to a lower amplification of the output signal elicited by copper ions. The World Health Organization (WHO) sets the maximum allowable concentration of copper ions in drinking water at 2 mg/L (about 30 μM), while China's standard is 1 mg/L (about 15 μM). Therefore, it's important for a copper biosensor to be more sensitive at concentrations around 10 μM and below. Current biosensors using the CueR system only show a 2-fold increase in signal at a concentration of 1 μM Cu(II), and just 7-fold at 10 μM[20]. Another approach to improve copper sensors involves creating a sensitive bioreporter by integrating cop-operon sensing elements and using

[1]School of Chemistry, Northeast Normal University, Changchun, Jilin, China. [2]State Key Laboratory of Electroanalytical Chemistry, Changchun Institute of Applied Chemistry, Chinese Academy of Sciences, Changchun, Jilin, China. [3]School of Applied Chemistry and Engineering, University of Science and Technology of China, Hefei, Anhui, China. [4]Department of Chemistry and Physics, State University of New York at Stony Brook, Stony Brook, NY, USA.
✉e-mail: fangxn482@nenu.edu.cn

gene knockout techniques. The best result so far is an 18-fold signal increase at 100 μM and a 15-fold increase at 10 μM, achieved by knocking out the *copA* gene[13]. However, during actual detection, factors like signal interference and instrument limitations can introduce significant errors. The challenge of enhancing the fold-change (the ratio of the fluorescence intensity after adding Cu(I) to that before addition) poses a significant obstacle in the practical application of biosensors, as low multiples of signal changes hamper our ability to assess signal authenticity.

The two-component system recognizes a wider range of inputs, making it advantageous for biosensor development. This compensates for single-component biosensor limitations, providing unparalleled benefits in synthetic biology. Phosphorylation and dephosphorylation processes within this system amplify response signals, making CusRS-based biosensors a promising strategy to overcome weak signal responses. Despite prior reports, their sensitivity and detection thresholds have yet to surpass expectations. A copper ion biosensor based on CusRS system was designed with P_{cusC} as its promoter. The limit of detection (LOD) for copper ions in this system was 26 μM, with a 5-fold signal enhancement at 1 mM Cu(II)[21]. An improved copper ion sensing system was created by adding a positive feedback loop, resulting in a lower detection threshold of 4 μM and a 1.5-fold increase in signal strength at 10 μM. Even at high concentrations of 1 mM, the signal enhancement reached merely 7-fold[22]. Additionally, a biosensor using the CopRS system (a CusRS-like system) and betaxanthin as a signal output, showed a fold-change of 16 at 1 mM[23]. Another biosensor integrating the CusRS system with a cell-cell communication module had a high detection limit at 12 μM, indicating minimal improvement[24].

Previous studies showed the CusRS system couldn't notably boost induction at low copper levels, underperforming compared to CueR-based sensors, making it hard to meet WHO detection standards. Here, we improved cusRS-based biosensors by adjusting CusRS levels, introducing signal amplifiers, and removing copper detox genes *cueO* and *cusCFBA*, achieving a fold-change of 18 at 1 μM, which increased up to ~100-fold by optimizing cell culture procedure. We proposed innovative testing and analysis methodologies, making detection easier and more efficient, significantly lowering the detection threshold. Our discourse endeavored to furnish pertinent insights for investigations into other two-component systems and biosensors, thereby augmenting our comprehension of such systems in forthcoming research.

Results

Sensors based on CusRS two component system

The bacterial CusRS two-component system primarily regulates copper homeostasis. As depicted in Fig.1A, copper ions bind to the periplasmic sensor domain of CusS, initiating autophosphorylation. Phosphorylated CusS engages with CusR, facilitating the transfer of the phosphate group to CusR, activating the promoters P_{cusC} and P_{cusR}, consequently up-regulating the expression of CusSR and CusCFBA. This implies that the CusR production is boosted by CusR-P, creating a positive feedback loop. Concurrently, the CusCFBA complex expels copper ions from both cytoplasm and periplasm space to maintain cellular homeostasis. To assess the copper-sensing capability of endogenous CusS located on the chromosome of *E. coli*, we evaluated the response of the strain SX1747 (Fig.1B) to varying concentrations of copper (Fig.1C). Here, SX1747 is a K12 strain with CusS labeled by YFP on chromosome which comes from the *E.coli* Genetic Stock Center[25]. We measured the response of SX1747 to Cu(II) using the flowing procedure: The overnight bacterial culture was diluted with fresh LB medium at a 1:100 ratio and incubated until the $OD_{600} \approx 0.6$. The culture was then induced with varying concentrations of Cu(II) for 5 h before analysis. However, we observed only a minimal fluorescence signal, even at a high concentration of 100 μM (Fig. S1A and Fig.1C). These findings suggested that P_{cusC} acted as a weak promoter, and the native CusRS system's response in *E. coli* was suboptimal for copper detection. This inadequacy might also explain why most previously reported copper sensors did not employ CusRS systems.

To enhance the sensor's performance, we engineered a positive feedback circuit plasmid, pCWCu32, with *cusR* and superfolder green fluorescent protein (sfGFP) downstream of the P_{cusR} and P_{cusC} promoters, respectively (Fig.1B). Upon comparing with SX1747, we performed the same measurement and observed a tenfold LOD reduction from 10 μM to 1 μM in Cu32. However, the output signal increased only 1.9-fold at 10 μM, and 2.2-fold even at a high Cu(II) concentration of 100 μM, which was just marginally better than SX1747 (Fig. S1B, S1C and Fig.1C). There were two reasons here that may have contributed to improved detection. On the one hand, a higher copy number on plasmid could increase protein expression, thereby enhancing the output signals. Another more important reason was that the introduction of an additional *cusR* gene on plasmid would increase its expression in cells, and thus promoted the positive feedback of CusR on the promoter, leading to a decrease in LOD and an increase in fluorescence signal. The results indicated that the overexpression of CusR could increase output signal and optimize detection performance.

Although the detection performance of Cu32 exhibited a marginal improvement, the fluorescent signal from the test results remained weak, and the sensitivity of the biosensor was still low. We could only observe a fold-change (I/I_0) of 1.9-fold at 10 μM. To further increase the output signal, we modified pCWCu32 by introducing a *repL* gene upstream of *sfGFP* to create the plasmid pCWCu1. The *repL* gene contains its own replication

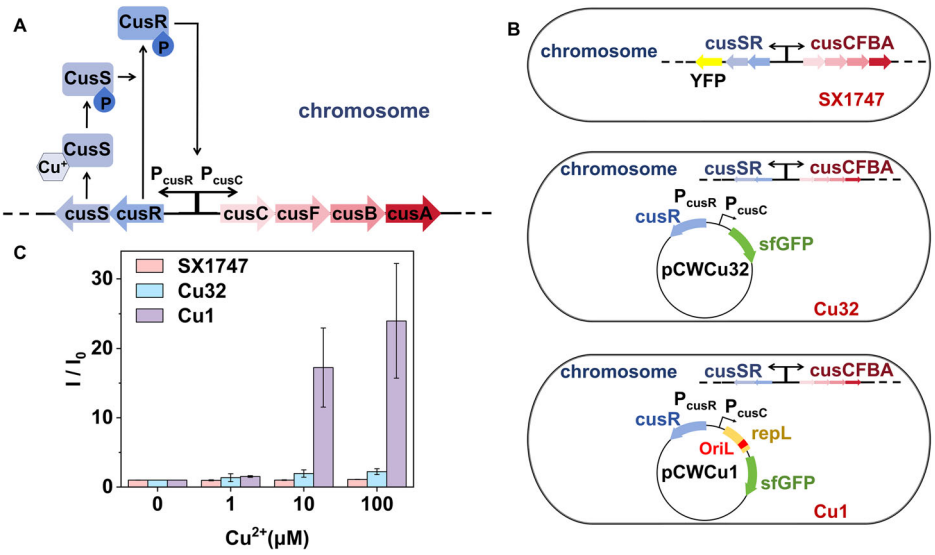

Fig. 1 | Cu(II) biosensors based on the CusRS two component system and their characterization of response to Cu(II). A Schematic diagram of the CusRS two component system on *E. coli* chromosome. **B** The schematic diagram of the genetic elements of constructed Cu(II) biosensors Cu1, Cu32 and SX1747. **C** Comparison of the fold-change (I/I_0) for Cu32, SX1747 and Cu1 at different concentrations of Cu(II). All measurements were conducted with $n = 3$ independent replicates. Error bars represented the standard deviation of $n = 3$ independent replicates.

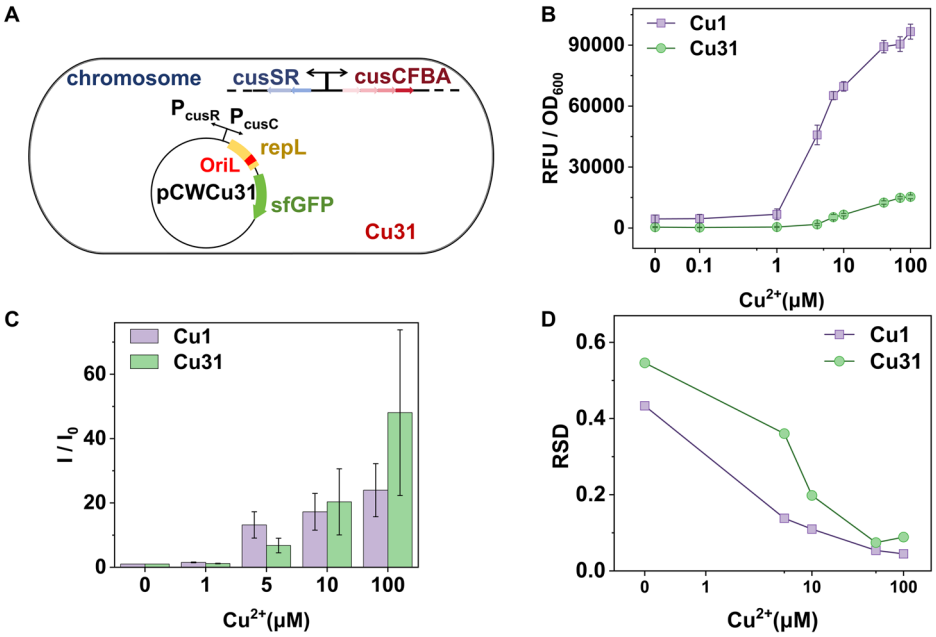

Fig. 2 | The role of CusR in the CusRS two component system based biosensor. A The schematic diagram illustrated the genetic elements of the constructed Cu(II) biosensor, Cu31. **B** Dose-dependence of biosensors Cu1 and Cu31 to different concentrations of Cu(II). **C** The comparison of the fold-change (I/I_0) for biosensors Cu1 and Cu31 across various concentrations of Cu(II). These measurements were replicated independently $n = 3$ times, and the error bars denoted the standard deviation. **D** Stability comparison of Cu1 and Cu31 by plotting the relative standard deviation (RSD) and the measurement was performed with $n = 10$ independent replicates.

origin (oriL), which is activated by the RepL protein. As shown in Fig. S2, in the presence of Cu(II), the P_{cusC} promoter is activated, resulting in elevated expression of protein RepL, thereby increasing the plasmid's copy number. This increase in plasmid copy number, coupled with the direct increase in sfGFP expression, significantly amplifies the overall sfGFP signal[26]. We compared the responses of strains SX1747, Cu32 and Cu1 to varying concentrations of Cu(II) under the same experimental conditions as described for testing SX1747. (Fig. 1C and Fig. S1D). The results indicated that the introduction of *repL* significantly amplified the fluorescent signal. Although the LOD remained largely unchanged, there was a substantial increase in responsive signal, thereby greatly enhancing Cu(II) biosensor sensitivity (Fig. S1D). As shown in Fig. 1C, the fold-change (I/I_0) in Cu1 exceeded 17-fold at 10 μM and approached 24-fold at 100 μM of Cu(II), which was significantly higher than that in SX1747 and Cu32. However, we only observed a weak signal enhancement at 1 μM with a fold-change (I/I_0) of 1.5-fold. Our results indicated that the natural sensing capability of CusRS system in *E. coli* for Cu(II) ions was insufficiently robust, rendering them ineffective as copper sensors. Nonetheless, we demonstrated that it was possible to enhance their sensitivity by incorporating a signal amplifier and overexpressing *cusR* on a plasmid.

The roles of CusR in the Cu(II) biosensor based on the CusRS two component system

As noted above, CusR is pivotal in the CusRS-based Cu(II) biosensor, likely enhancing the sensor's functionality by amplifying output signals and diminishing the LOD. To substantiate CusR's impact on the biosensor, we engineered the plasmid pCWCu31 by excising *cusR* gene from pCWCu1, thereby creating the Cu31 sensor (Fig. 2A). Subsequently, we explored the contributions of CusR to the sensor's performance by comparing Cu1 and Cu31.

We compared the responses of Cu1 and Cu31 to various concentrations of Cu(II), using identical experimental conditions as those described for testing SX1747. The absolute fluorescence intensities in Fig. 2B indicated that the output signals in Cu1 were significantly enhanced due to the introduction of additional CusR, suggesting its activation effect. However, it was noteworthy that the background signal, which is the fluorescence intensities in the absent of Cu(II), also increased remarkably. This increase likely originated from the cross-talk phosphorylation of CusR by other kinases[27,28], overexpressing of CusR amplified this cross-talk effect. This suggested that overexpression of CusR could not only increase the output signal, but also the basal noise. Examination of the fold-change (I/I_0) under a series of Cu(II) concentrations revealed that the value of I/I_0 for Cu1 was higher than that for Cu31 at low concentrations of Cu(II) (Fig. 2C). It was demonstrated that the sensitivity of Cu1 exceeded that of Cu31 at low concentrations of Cu(II). An observable increase in the ratio I/I_0 was evident at 1 μM in Cu1 (1.5-fold), but not for Cu31, confirming that an increase in CusR could indeed reduce LOD of sensors to a certain degree. However, it was important to highlight that the response of I/I_0 for Cu1 was actually inferior to that of Cu31 at high concentrations of Cu(II). This might be attributed to the nonlinear relationship between fluorescence intensity and concentration, particularly when the quantity of sfGFP in cells exceeded a certain threshold[29]. Nonetheless, the entirety of the results unequivocally confirm that CusR enhanced the sensitivity of CusRS-based Cu(II) biosensors, especially within the low Cu(II) concentration range (≤10 μM).

Stability is a critical factor to consider in the development of biosensors. To evaluate this, we tested and assessed the stability of the biosensors. For sensors Cu1 and Cu31, we picked 10 single colonies from LB plates and measured them with the same procedure (Fig. S3B and S4B). Then the average fluorescence intensity and standard deviation (SD) of the 10 parallel data for Cu1 and Cu31 were calculated respectively. The relative standard deviation (RSD) was then obtained by dividing the standard deviation by the average fluorescence intensity, as illustrated in Fig. 2D. As observed, the RSD of Cu1 was consistently lower than Cu31 across the entire detection range, indicating a higher stability of Cu1. This enhanced stability of Cu1 could be attributed to two main factors. Firstly, CusR overexpression might have improved the sensor's response, thereby reducing the fluctuation in responses between cells. And on the other hand, the fluorescence intensity of Cu1 was substantially higher than that of Cu31, and the microplate reader might performance better at higher fluorescence levels, reducing error in low-signal detection.

Our comparative analysis of Cu1 and Cu31 revealed that an elevation in the expression level of CusR augmented the output signal of the biosensors, especially increased the fold-change (I/I_0) at low concentrations, lowered LOD and improved stability of the biosensor as well. However, we also saw a significant increase in the background noise, which adversely affected the development of an optimal biosensor.

The roles of CusS to CusRS two component system based biosensors

CusS constitutes another principal element of the CusRS system. In an effort to elucidate the influence of CusS on the Cu(II) biosensing capabilities of the CusRS two-component system, we engineered a series of sensors-Cu18, Cu27 and Cu33-each distinguished by differential expression levels of CusS. As depicted in Fig. 3A, the *cusS* gene was inserted downstream of *cusR* in plasmid pCWCu1 to generate plasmid pCWCu18. Subsequently, pCWCu18 was transformed into the host strain *DH5α* to obtain the Cu18 sensor. Plasmids pLC8 and pLC17 were constructed by introducing an additional *cusS* gene under the control of the constitutive promoters *BBa_J23109* and *BBa_J23100*, respectively. The plasmid pCWCu1 was co-transformed with pLC8 and pLC17 into the host strain *DH5α* to generate the sensors Cu27 and Cu33, respectively. Subsequently, the responses of sensors Cu1, Cu18, and Cu27 were evaluated using the same testing procedure as those mentioned above for testing SX1747. As illustrated in Fig. 3B, the output signals of Cu18 and Cu27 were consistently observed to be weaker than those of Cu1. Furthermore, the background fluorescence in the absence of Cu(II) in these sensors was also diminished in comparison to Cu1. These findings suggested that the upregulation of CusS led to a decrease in the fluorescence of the biosensors, regardless of the presence of Cu(II). This reduction was potentially attributable to the phosphatase activity of CusS[27].

Subsequent analyses demonstrated that the sensors in Cu33, Cu27, and Cu18 displayed marked disparities in their response of to Cu(II). Specifically, *BBa_J23109* in Cu27 acted as a relatively feeble promoter, in stark contrast to *BBa_J23100* in Cu33, which functioned as a robust promoter with an efficacy approximately 20-fold greater than that of *BBa_J23109*. The expression level of CusS in Cu27 was significantly lower than that in Cu33. Furthermore, the results indicated a positive correlation between the degree of reduction in the output signal and the expression level of CusS in the cells. In the case of sensor Cu33, the signal was undetectable due to the excessive expression of CusS (Fig. S5C). Lower signal in Cu18, in comparison to Cu27, implied higher CusS expression, suggesting the promoter of P_{cusR} was stronger than *BBa_J23109*.

The results presented above indicated that the incorporation of CusR enhanced the output signal but also background noise, which posed a challenge for the development of highly sensitive sensors. Conversely, CusS reduced the response signal as well as the background noise. This leads to the question: Does CusS further improve the performance of sensors by reducing background noise, building upon the effects of CusR? To elucidate the influence of CusS on copper sensors and verify our hypothesis, we calculated the fold-change (I/I_0) for Cu1, Cu18, Cu27, and Cu33 across varying concentrations of Cu(II). As depicted in Fig. 3C, the observed values of I/I_0 for both Cu18 and Cu27 were consistently higher than those for Cu1 across all tested concentrations of Cu(II). This observation underscored the significantly enhanced sensitivity of Cu18 and Cu27 compared to Cu1. Notably, the fold-change (I/I_0) reached approximately 100-fold for Cu18 and 50-fold for Cu27 at a concentration of 10 μM, far surpassing those of all previously reported copper sensors. It was imperative to observe that an excessive concentration of CusS in Cu33 markedly diminished the output signal, consequently impairing the sensor's responsiveness. This indicated that CusR and CusS exerted antagonistic effects on the modulation of the output signal. Thus, enhancing the sensor's sensitivity could be achieved by judiciously modulating the concentration of CusS within a specified range.

To investigate the effect of CusS on sensor stability, we assessed the repeatability of sensors Cu18 and Cu27. We analyzed the data of I/I_0 collected over 4 different days for both Cu18 and Cu27, as illustrated in Fig. S5A and S5B, respectively. The results indicated a significant correlation between the fluctuations in CusS expression levels and the stability of the biosensor (Supplementary Note 1). To enhance the stability of the biosensor, it was advisable to express CusS under a constitutive promoter.

As a consequence, properly adjusting the expression levels of CusS and CusR could significantly improve the detection sensitivity of the sensors. Given that the functions of HK (like CusS) and RR (like CusR) are fundamentally similar in most two-component systems (TCSs), we posit that this strategy of enhancing the performance of TCS based biosensors through the balanced expression of CusR and CusS possesses broad applicability.

Optimize the performance of the sensor by knocking out genes associated with copper resistance

Both Cu18 and Cu27 exhibited a fold-change (I/I_0) up to several tens of times at a copper concentration of 10 μM. However, at lower concentrations (<1 μM), neither exhibited a significant signal response. To enhance the detection threshold and achieve a more effective Cu(II) biosensor with superior detection capabilities, it is imperative to lower the LOD and augment sensitivity. It is well known that CusCFBA in *E. coli* functions to transport copper ions from the cytoplasm and periplasmic space to the exterior of the cell. Another related protein, CueO, is capable of oxidizing Cu(I) to Cu(II) within the periplasmic space. Upon entering the cell, Cu(II) can be reduced to Cu(I) by certain reductases, such as NDH-2[30]. CusS binds to Cu(I) and undergoes self-phosphorylated, subsequently phosphorylating

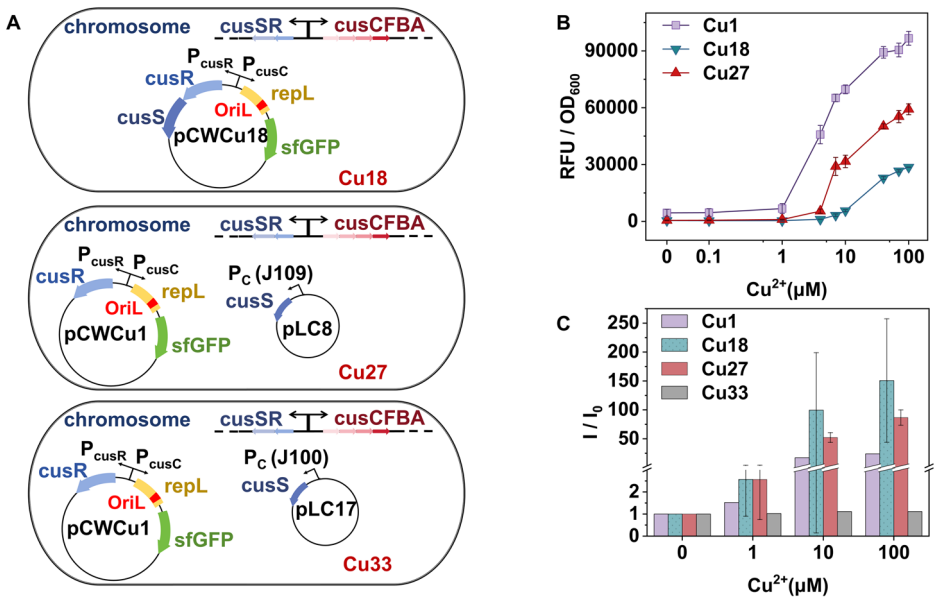

Fig. 3 | Exploring roles of CusS in the CusRS based Cu(II) biosensor by comparing the sensors with different CusS expression ability. A The schematic diagram of the genetic elements of constructed Cu(II) biosensors Cu18, Cu27 and Cu33. **B** Comparison of the responding curves to Cu(II) for sensors of Cu1, Cu18 and Cu27. The measurement was performed with $n = 3$ independent replicates, and error bars represented the standard deviation. **C** Comparison of the fold-change (I/I_0) for biosensors Cu1, Cu18, Cu27 and Cu33 at various concentrations of Cu(II). The measurements of Cu18 and Cu27 were tested on 4 different days with the same condition. Error bars represented the standard deviation of $n = 4$ measurements. In comparison, Cu27 exhibited lower variability in measurements, as indicated by a reduced standard deviation, suggesting higher stability.

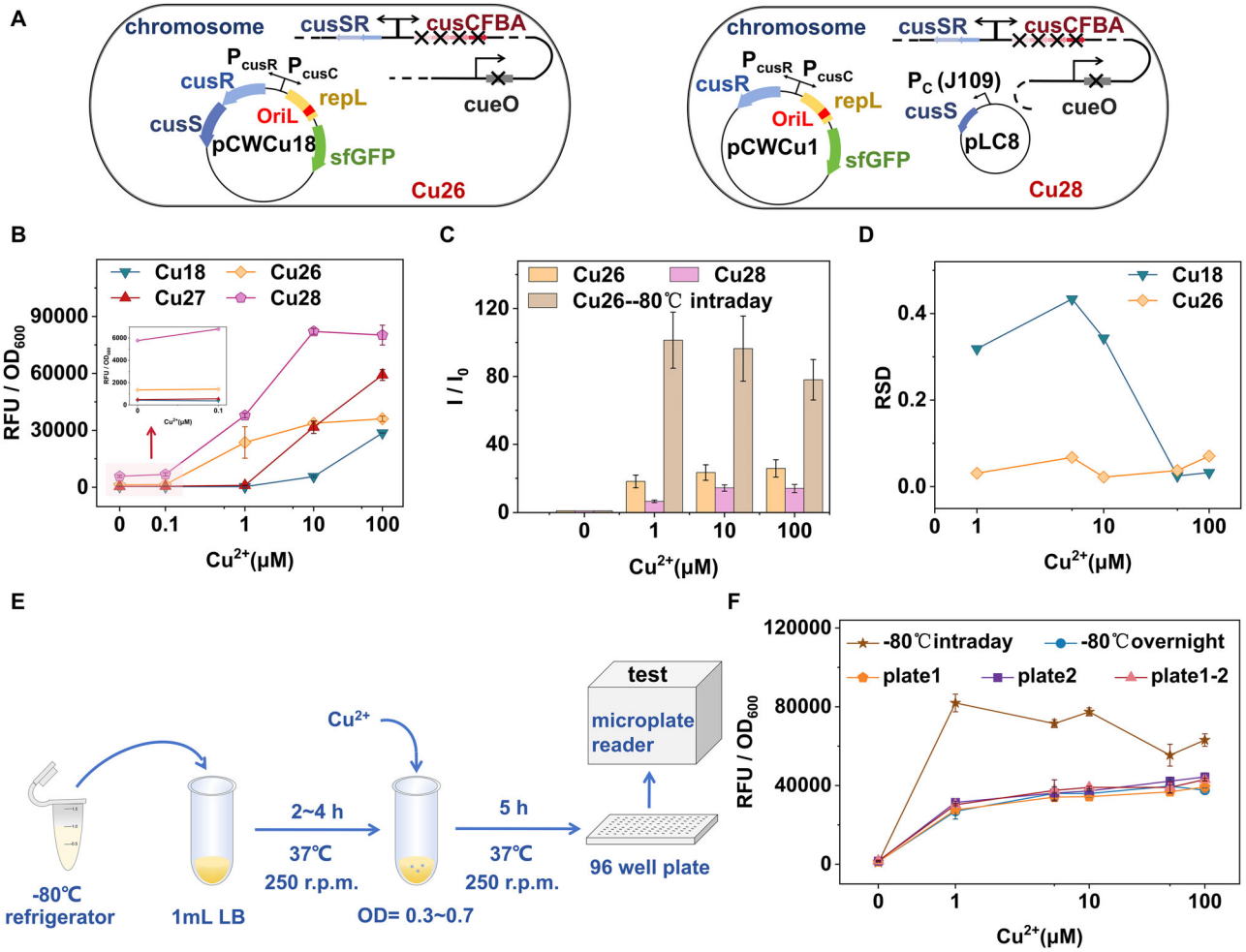

Fig. 4 | Improving characteristics of the sensors. A The schematic diagram of the genetic elements of constructed Cu(II) biosensors Cu26 and Cu28. **B** The responding curves of biosensors Cu18, Cu26, Cu27 and Cu28. The data at low concentrations were taken out and displayed in the inserted figures. **C** Comparison of the fold-change (I/I_0) for biosensors Cu26 and Cu28. And Cu26 included two sets of data tested under standard cell culture procedure (sample 'Cu26') and our proposed culture procedure (sample 'Cu26-80°C intraday'). **D** The relative standard deviation (RSD) of Cu18 and Cu26 across different concentrations of Cu(II). The measurement was conducted using $n = 8$ independent replicates. **E** The schematic diagram illustrating the experimental workflow for 'Cu26_−80 °C intraday'. **F** Response curves of Cu26 with different active states as described in Supplementary Note 2 and Fig. S10. All measurements in Fig. 4B, C and F were conducted with $n = 3$ independent replicates, and error bars represented the standard deviation.

CusR and activating promoters P_{cusR} and P_{cusC}[17]. Given that the CusRS system predominantly responded to Cu(I)[30], we conducted *cusCFBA* and *cueO* genes double knockout experiments in *E. coli DH5α* strains to enhance the cellular accumulation of Cu(I). Then the plasmid pCWCu18 was transformed into the double knockout strain, resulting in the sensor Cu26. Additionally, the plasmids pCWCu1 and pLC8 were co-transformed into the double knockout strain, leading to the development of the sensor Cu28 (Fig. 4A).

Subsequently, we assessed and characterized the properties of these two sensors. Initially, we compared the fluorescence output of Cu18, Cu26, Cu27, and Cu28 using the same testing procedure as those mentioned above for testing SX1747 (Fig. 4B). The findings revealed that the double knockout strains Cu26 and Cu28 demonstrated significantly higher fluorescence intensities compared to Cu18 and Cu27 at Cu(II) concentrations of 10 μM and below. Upon examining the basal intensity in the absence of Cu(II), we observed that the background signals of Cu26 and Cu28 were elevated in comparison with those of Cu18 and Cu27 (subgraph in Fig. 4B). Concurrently, we observed a LOD as low as 0.1 μM, approximately an order of magnitude lower than those observed for Cu18 and Cu27. By comparing the fold-change (I/I_0) for Cu26 and Cu28 which depicted in Fig. 4C, we observed an I/I_0 value of 18-fold for Cu26 and 7-fold for Cu28 even at 1 μM. However, at this concentration, merely weak signal responses were detected in Cu18 and Cu27 with both showing the I/I_0 value of only 2.5-fold (Fig. 3C). Meanwhile, the I/I_0 of Cu26 was higher than Cu28, indicating that Cu26 had superior sensitivity and response compared to Cu28. Consequently, it could be posited that Cu26 represented a significantly more optimal Cu(II) biosensor. On the other hand, considering the overexpression of CusRS could potentially impact on bacterial growth, we performed growth curve analyses comparing the engineered strain Cu26 to its parental strain (*DH5α::ΔcueOΔcusCFBA*) under conditions of 1 μM Cu(II) induction and non-induction, as the results depicted in Fig. S8. Our results indicated no significant difference in growth rates even under high expression of CusRS with 1 μM Cu(II) induction, suggesting that the overexpression of CusRS did not affect bacterial growth in our experimental setup.

The findings indicated that the double-knockout strains were capable of enhancing the output signal and the basal noise to a certain degree, concurrently decreasing the LOD of biosensors. This characteristic underscored a substantial benefit of employing double-knockout strains in the detection of low concentrations. This enhancement was likely due to the accumulation of more Cu(I) within cells due to the absence of proteins associated with copper efflux and oxidation.

As the previous results indicated, Cu18 exhibited the poorest repeatability, raising repeatability concerns of its derived sensor Cu26. To verify the stability of sensor Cu26, we initially performed parallel experiments by analyzing cells from eight distinct plaques, as depicted in Fig. S9. The response curves from these parallel experiments demonstrated a high degree of consistency, thereby revealing the acceptable repeatability of Cu26. Then we compared the RSD of Cu26 and Cu18 for the eight parallel experiments (Fig. S6B), with the findings presented in Fig. 4D. It was evident that the RSD of Cu26 was lower, indicating enhanced stability of Cu26 compared to Cu18. This improvement may be attributed to the increased background signal in the absent of Cu(II) caused by the dual knockout of *cusCFBA* and *cueO* in Cu26, which reduced instrument detection errors and led to decrease fluctuations in the basal signal, thereby enhancing repeatability.

Due to the signal transduction mechanisms of two-component systems, which involve phosphorylation and dephosphorylation processes closely associated with intracellular ATP, the performance of sensors may be influenced by the metabolic activity status of cells. This influence potentially compromises the stability of cell-based biosensors. To assess stability across varying metabolic activity statuses, we compared the output signal of Cu26 under different cell viability. The schematic diagrams illustrating the experimental workflow to acquire sensor cells with different activity are presented in Fig. 4E and Fig. S10, with a detailed description provided in Supplementary Note 2. The bacterial cells of Cu26 strain from −80 °C frozen stock were re-incubated for varying times and durations to obtain samples with different metabolic activity level. Inoculated -80°C frozen bacteria (Fig. 4E) or diluted (1:100) overnight cultures with different metabolic activities (Fig. S10) were grown in fresh LB medium to the exponential phase. The cultures were subsequently induced with varying concentrations of Cu(II) for 5 h prior to fluorescence measurement. The results presented in Fig. 4F revealed that, with the exception of the 'Cu26_ −80 °C intraday' sample, all samples displayed remarkably similar responses. This suggested that stability of sensor Cu26 was robust as long as bacteria cells were inoculated from −80 °C stocks for more than one night and then re-inoculated, regardless of the duration of re-culturing. Furthermore, it was confirmed that loss of *cueO* and *cusCFBA* could enhance stability of the sensor. However, it was observed that 'Cu26_ −80 °C intraday' revealed significant different results compared to others. Furthermore, to examine the kinetics of the sensor response over time and gain a more comprehensive understanding of our sensor's features, we conducted experiments to measure the sensor's response at multiple time points (1, 3, 5, and 7 h) under different Cu(II) concentrations, as illustrated in Fig. S11. The results indicated that the temporal evolution of Cu26 exhibited a consistent trend across all tested concentrations: The sensor's response increased over time until 3 h of incubation with Cu(II), followed by a slight decrease under high concentration. This suggested that 3 h may be an optimal detection time point. Notably, within the 3–5 h detection window, the sensor's response showed minimal variation, demonstrating high temporal stability.

As illustrated in Fig. 4F, 'Cu26_ −80 °C intraday' exhibited a markedly higher output signal. When we took look at the value of I/I_0, we saw a signal multiplier of I/I_0 up to ~100-fold at the low Cu(II) concentration of 1 μM, surpassing all others significantly (Fig. 4C). This discovery suggested that we had developed a more optimized cell culture procedure for biosensors based on two-component system, resulting in signal responses significantly superior to those obtained through the standard culture procedures described in prior studies.

To verify the universality of this culture procedure for obtaining high sensitivity, we replicated the experiment described in Fig. 4F with sensors Cu1, Cu31, Cu18, and Cu27. The results, as illustrated in Figs. S3A, 4A, 6A, and 7A, were remarkably similar, low activity bacterial cells directly inoculated from −80 °C stocks, exhibited an extremely higher sensitivity in all the sensors. This enhancement might be attributed to the slower growth rate of low-active cells, leading to a rapid accumulation of intracellular sfGFP. Concurrently, by adopting this cultivation and detection methodology, we significantly reduced the measurement time and simultaneously improved detection efficiency, which is a feat not previously reported in the literature.

In conclusion, the double knockout strain Cu26 demonstrated a lower LOD, enhanced response sensitivity, an exceptionally high fold-change (I/I_0) at low concentrations of Cu(II), and improved stability. These attributes established it as a more optimal Cu(II) biosensor. Meanwhile, the fold-change (I/I_0) was as high as 100-fold at 1 μM, markedly surpassing all existing Cu(II) microbial sensors. We are confident in the potential for further enhancements to its performance.

Developing test and analysis methods to improve detection performance and capabilities

In the CusRS system, phosphorylated CusR can activate the promoters P_{cusC} and P_{cusR} simultaneously. To augment the fluorescence intensity, an additional gene encoding *sfGFP* was integrated downstream of *cusR* in pCWCu1, resulting in the plasmid pCWCu44. We then transformed the pCWCu44 into the wild type and double knockout strain of *DH5α* respectively to obtain the sensors of Cu44 and Cu47 (Fig. 5A). We tested Cu44 and Cu47 sensors using the same procedure as 'Cu26_ Fig.−80°C intraday' in Fig. 4E, aiming to achieve stronger output fluorescence signal. As illustrated in Fig. S12A and Fig. 5D, the fluorescence intensity of Cu44 and Cu47 indeed enhanced greatly comparing with Cu1, aligning with our expectations. The LOD for Cu47 was notably lowered by removing *cueO* and *cusCFBA* genes, and the fluorescence intensity for Cu47 was significantly greater than Cu44, especially at low concentration of 0.1 μM–1 μM.

Upon observation, it was discerned that when the fluorescence intensity surpassing the threshold of approximately 150,000 RFU/OD_{600}, the green coloration of sfGFP could be visually observed in the centrifuged cells (Fig. S12B). We then compared the centrifuged cells of sensor Cu47, both in the presence and absence of Cu(II). Notably, the samples containing Cu(II) exhibited a distinct green hue at 1 μM under the nature light (Fig. 5B). This confirmed that visual inspection can be used to detect Cu(II) without the need for detection instruments. The strategy facilitated straightforward and rapid detection of copper ions with minimal equipment requirements. While natural light allowed for basic detection, optimal visualization was achieved using a simple, low-cost 470 nm light source. Samples excited at 470 nm displayed significantly stronger fluorescence signals, enhancing the contrast and making the results more easily distinguishable by the naked eye (Fig. 5C). This innovative approach renders the biosensor detection of Cu(II) more efficient, straightforward, cost-effective, and user-friendly. It is particularly useful for applications that do not require highly precise detection, as well as for qualitative and semi-quantitative analyses.

We measured the expression of Cu47 at varying concentrations of Cu(II) via flow cytometry, with the results presented in Fig. S12C. It revealed two distinct peaks, indicative of low and high sfGFP expression respectively, and the expression distribution altered concomitantly with changes in Cu(II) concentration. As Cu(II) increased, the proportion of high-expression peaks increased while the proportion of low-expression peaks decreased. Finally, at sufficiently high concentrations of Cu(II), the peaks transitioned to a unimodal distribution and exhibited a rightward shift.

In light of these observations, we established an analytical method predicated on distribution data. We calculated the ratios of the proportion of low peak P_L to high peak P_H (P_L/P_H) as depicted in Fig. 5E. A noticeable change was observed in the P_L/P_H ratio at a Cu(II) concentration of 0.01 μM. It suggested that this data analysis method enabled a tenfold reduction in the LOD for the same sensor, compared to the traditional method of directly measuring the average signal output. Using this approach, we successfully developed the sensor Cu47, achieving a low LOD at 0.01 μM, which was an order of magnitude lower than previously reports[21,22]. Looking forward, we believe that this analysis method can also be applied to other biosensors utilizing a two-component system or those characterized by bimodal output signal data, with the aim of enhancing their detection capabilities.

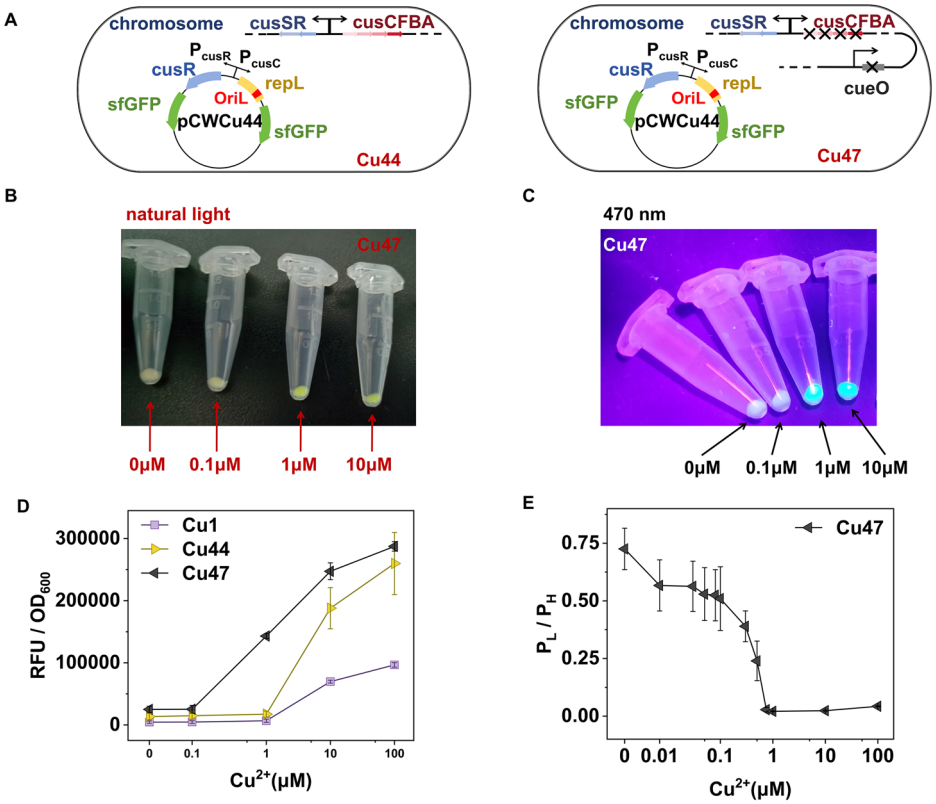

Fig. 5 | The improved test and analysis methods of Cu(II) biosensors based on two component system. A The schematic diagram of the genetic elements of constructed Cu(II) biosensors Cu44 and Cu47. **B**, **C** A centrifugally visible detection method to test Cu47 response to various concentrations of Cu(II), specifically at 0 μM, 0.1 μM, 1 μM and 10 μM, under natural light and 470 nm excitation light source. **D** Response curves of biosensors Cu1, Cu44 and Cu47 to different concentrations of Cu(II). The measurement was performed with $n = 3$ independent replicates, and error bars represented the standard deviation. **E** An improved analysis method of Cu47 to obtain lower LOD by calculating P_L/P_H at different concentrations of Cu(II), where P_L and P_H indicated the proportion of low and high fluorescence intensity peaks in Fig. S12C respectively.

The sensor of Cu(II) based on CusRS system exhibited much better sensitivity and selectivity than that of CueR system

In *E. coli*, the CueR system was commonly used to construct Cu(II) biosensors, which has demonstrated a lower detection limit than CusRS-based sensors in previous studies[31]. In this system, copper ions bind to CueR, activating the promoter P_{copA} to initiate the gene expression downstream (Fig. 6A). Here, we constructed a Cu(II) biosensor leveraging the CueR system for comparison with Cu26. As depicted in Fig. 6B, *sfGFP* gene was inserted downstream of P_{copA}. Additionally, a *repL* gene was introduced upstream of *sfGFP* to amplify the signal, thereby enhancing the accuracy of comparison, resulting in the plasmid of pMT010. The CueR system predominantly responds to cytoplasmic copper ions, whereas CopA plays a crucial role in the expulsion of copper ions from the cytoplasm. To improve its sensitivity[31], the plasmid of pMT010 was transferred into the a *copA* gene knock-out strain of *DH5α*, generating the Cu-cueR1 sensor. We then compared the responses of the sensors Cu26 and Cu-cueR1 (Fig. 6C and Fig. S13A). As illustrated in Fig. 6C, the fold-change (I/I_0) of Cu26 was significantly higher than that of Cu-cueR1, demonstrating that biosensors based on two-component system exhibited superior response sensitivity.

Then, to investigate the selectivity of Cu26, we evaluated the fold-change (I/I_0) in the presence of various heavy metal ions at a concentration of 5 μM under our newly proposed culture procedures. As the results presented in Fig. 6D, the I/I_0 values of Cu26 were 0.79 for Co^{2+}, 0.77 for Hg^{2+}, 0.96 for As^{3+}, 0.79 for Zn^{2+}, 1.03 for Fe^{3+}, 1.04 for Ag^{+} and 81.26 for Cu^{2+}, which were all close to 1 excluding Cu(II), thereby demonstrating the outstanding selectivity of the sensor Cu26. Upon observation, it was noted that Cu26 exhibited no response to Ag(I), despite previous reports indicating that CusS harbored binding sites for Ag(I)[27,32]. This might be due to excessive CusS enhancing its phosphate activity, thereby reducing the output signal. Meanwhile, the selectivity of biosensor Cu26 under standard cell culture procedure was also evaluated, as reflected in Fig. S14. The results demonstrated excellent selectivity, further confirming the high specificity of Cu26 for copper ions.

Given that previous reports have indicated that CusR can also be phosphorylated by another kinase, YedV, in response to H_2O_2, potentially leading to signal cross-talk[33], it is essential to verify whether this cross-talk would affect the selectivity of the sensor. Therefore, we conducted specific experiments to test the response of biosensor Cu26 to H_2O_2. As illustrated in Fig. 6E and Fig.S15, we investigated the response of Cu26 to high concentrations of H_2O_2 (0.5 mM–6 mM) under both our proposed and standard cell cultural procedure. The results indicated that H_2O_2 could indeed activate the CusRS system, though the response signal was minimal. Even at the highest concentration of 6 mM H_2O_2, the fold-change of I/I_0 was only 1.5-fold to 5-fold, which was substantially lower than that responds to Cu (II) as shown in Fig. 4C (with I/I_0 exceeding 20-fold under standard cultural condition and approximately 100-fold under newly proposed culture condition). This demonstrated that Cu26 exhibited negligible signal response to H_2O_2, indicating that potential crosstalk does not significantly affect the detection specificity of the sensor.

Discussion

Microbial sensors offer unparalleled benefits for rapid detection and early warning of biological toxicity in water. Nevertheless, previously reported Cu(II) microbial sensors didn't show significant signal enhancement at low concentrations of Cu(II). They exhibited a fold-change of merely 2-fold at 1 μM[20] and 15-fold at 10 μM[13], severely limiting their practical applications. In this study, we conducted investigation into the CusRS-based biosensor, elucidating the roles of CusR and CusS in the sensor. Our results demonstrated that CusR significantly enhanced both the background and overall signal of the biosensors. Conversely, CusS was found to have an inhibitory effect, reducing both the basal and overall output signals. This discrepancy may be ascribed to the bifunction of CusS, which possesses both histidine kinase and phosphatase activities, facilitating the phosphorylation or dephosphorylation of CusR. Accordingly, the precise regulation of CusR and CusS expression levels is imperative for the successful development of a Cu(II) biosensor leveraging the CusRS system. Following the initial development, we engineered a suite of Cu(II) biosensors leveraging this

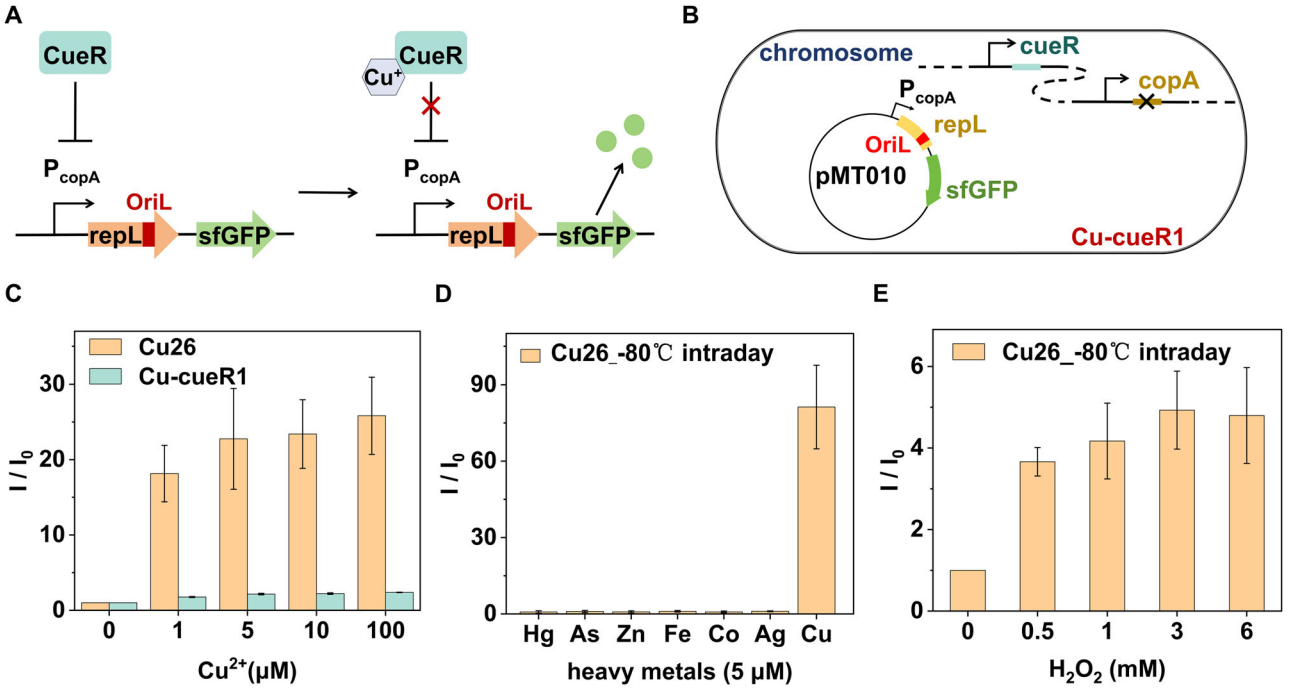

Fig. 6 | The comparison of Cu(II) biosensors based on the CueR system and the CusRS system. A Schematic diagram of the CueR system. **B** The schematic diagram of the genetic elements of constructed Cu(II) biosensor Cu-cueR1. **C** Comparison of the fold-change (I/I_0) for biosensors Cu26 and Cu-cueR1. **D** The selectivity of Cu26. The fold-change (I/I_0) of Cu26 for various heavy metals was determined at a concentration of 5 μM using our proposed '−80 °C intraday' procedure. **E** Response of Cu26 to H_2O_2 at '−80 °C intraday' using our proposed '−80 °C intraday' procedure. All test conditions adhered to conventional method: an overnight bacterial culture was diluted 1:100 in fresh LB medium and grown to $OD_{600} \approx 0.6$, then exposed to Cu(II) for 5 h. This analysis was conducted using $n = 3$ independent replicates, with error bars indicating the standard deviation.

framework, which demonstrated superior efficacy. This was achieved by modulating the expression levels of CusS/CusR and employing a double knockout strategy for the *cueO* and *cusCFBA* genes. The optimized biosensor showcased an impressive detection threshold of merely 0.01 μM, coupled with exceptional stability and sensitivity. Significantly, at low Cu(II) concentrations (≤10 μM), our biosensors Cu18, Cu27, and Cu26 demonstrated substantially higher fold-change (I/I_0) than previous studies. Furthermore, by refining the cell culture protocol, we were able to amplify the output signal, achieving a fold-change of 100-fold for Cu26 at 1 μM. Equally notable, the optimal cell culture procedure not only enhanced the sensitivity but also reduced the bacterial culture time to approximately 3 h, significantly faster by tens of hours compared to the normal culture procedure. Finally, given the observation that phosphorylated CusR could concurrently activate the promoters P_{cusR} and P_{cusC}, the output signals were further enhanced by incorporating *sfGFP* downstream of both promoters. Armed with these innovative sensors, color changes of the sensor could be observed with the naked eye at concentrations of Cu(II) of 1 μM or higher. This advancement broken the sensors' reliance on instrumentation, significantly broadened their application scope, and further reduced detection costs. We posit that considerable potential remains for further exploration of the CusRS system and eagerly anticipate future research endeavors. Our research also provides valuable reference points for subsequent investigations into related sensor types or other two-component systems.

Experimental methods

Strains, reagents and growth medium

Plasmid construction, biosensor detection and gene knockout were all performed in *E. coli DH5α* (Solarbio, C1100). SX1747 is a K12 strain with CusS labeled by YFP on chromosome which comes from the *E.coli* Genetic Stock Center[25] (Yale University, New Haven). Cells were cultured in fresh Lysogeny Broth (LB) medium supplemented with the appropriate antibiotics. The LB medium comprised 1 g of yeast extract, 2 g of tryptone, and 2 g of sodium chloride, dissolved in 200 ml of deionized water. This mixture was then autoclaved at 121 °C for 15 min. The antibiotic concentrations employed for strain selection were as follows: 50 μg/ml for ampicillin (Cat: A1170), 50 μg/ml for kanamycin (Cat: K1030), 50 μg/ml for spectinomycin (Cat: S8040), and 10 μg/ml for chloramphenicol (Cat: C8050), as applicable. Tryptone, yeast extract, sodium chloride, agar, kanamycin, ampicillin, spectinomycin and chloramphenicol were purchased from Solarbio. $CuCl_2 \cdot 2H_2O$ was purchased from Xilong Scientific Co. LTD (Guangdong, China). The phosphate buffered saline (PBS,1X) was purchased from Servicebio.

Testing conditions

For the characterization of biosensors, single colonies were selected and inoculated into 5 ml of LB medium supplemented with the appropriate antibiotic overnight (about 14–16 h) at 37 °C and 250 r.p.m. in a shaker (ISRSD3). Then the next day, the cells were diluted (1:100) in fresh LB medium and continuous shaking (250 r.p.m.) at 37 °C until OD = 0.5–0.7 (about 2.5–3 h). Next we added a series of different concentration gradient $CuCl_2$ solution to the bacteria cultures and incubated about 5 h for detection. The right volume of $CuCl_2$ dilutions were added to make sure the final concentration of 0.1, 1, 4, 5, 7, 10, 40, 50, 70, 100 μM. Afterward, we collected 500 μl bacteria cultures for centrifuge 1 min at 12,000 *g*, then washed and resuspended in 1.5 ml PBS. Finally, we added 200 μl dilute samples to the 96 well plate for measuring by microplate reader (TECAN, Spark) and analyzed using the SPARKCONTROL Dashboard software. We set the absorbance at 600 nm (OD_{600}) to obtain the cell density. And the excitation wavelength we set was 475 nm, meanwhile the fluorescence signal of superfold green fluorescent protein (sfGFP) was collected and recorded between 505 nm and 560 nm. For the medium background, we measured the PBS at every experiment, and also measured the wild type *DH5α* bacteria as a negative control.

We also measured by flow cytometry to obtain the data at the single cell level and analyzed using FlowJo 10.8.1 software. Each sample collected data on 30,000 bacterial cells, and utilizing preliminary forward scatter (FSC) and

side scatter (SSC) gating to exclude debris and identify the initial cell population. For the other test method, cells were directly inoculated with LB medium from −80 °C refrigerator and cultured with the same condition until OD = 0.3–0.7. Following this, Cu(II) was added and incubated for 5 h before test. Subsequently, 1.5 ml cell cultures were collected by centrifuging, then observed cells color and took pictures as a result. In this paper, all results were obtained under standard culture procedure unless explicitly stated otherwise.

Construction of plasmid and bacterial strains

We employed standard molecular biology methods to construct all plasmids utilized in this study. Details regarding the plasmids, strains, and primers used were summarized in Supplementary Table 1, Supplementary Table 2, Supplementary Table 3 and Supplementary Table 4, with confirmation obtained through sequencing (Comate Bio, Jilin, China). First, the vector containing *repL* and *sfGFP* genes was amplified from the pXYHg5 (in lab) by polymerase chain reaction (PCR) using primer pair F1:R1. And the insert containing *cusR* fragment and its promoter P_{cusR}-P_{cusC} was amplified from *E. coli* K12 MG1655 chromosome using primer pair F2:R2 by PCR. Then, through the restriction enzymes (*Ecor* I/*Sal* I) digestion and ligation by T4 ligase pCWCu1 (*pXW109Hg-cusR-*P_{cusR}*-*P_{cusC}*-repL-RBS-sfGFP*) was constructed. With the same method, pLC8 (*pSB1C3-J109-cusS*) was constructed by ligation using pLC4 (in lab) for *BBaJ23109* promoter and *cusS* fragment from *E. coli* K12 MG1655 chromosome. Based on pLC8, we changed *BBaJ23109* promoter to *BBaJ23100* promoter to construct pLC17 (*pSB1C3-J100-cusS*). We used another ligation method to obtain pLC17, which could directly connect using the vector fragment and insert fragment containing the same residue (about 20nt) as the vector at either side. Meanwhile we used pCWCu1 as template to insert *cusS* fragment. After that, we inserted another fragment *sfGFP* on this basis, thus pCWCu18 (*pXW109Hg-cusS-cusR-*P_{cusR}*-*P_{cusC}*-repL -RBS-sfGFP*) and pCWCu44 (*pXW109Hg-sfGFP-cusR-*P_{cusR}*-*P_{cusC}*-repL-RBS-sfGFP*) were constructed. In addition, the control plasmids pCWCu31 (*pXW109Hg-*P_{cusR}*-*P_{cusC}*-repL-RBS-sfGFP*) and pCWCu32 (*pXW109Hg-cusR-*P_{cusR} *-*P_{cusC}*-sfGFP*) were obtained by PCR (F3:R3, F4:R4) using pCWCu1 as template.

To enhance the performance of biosensors, we also modified the *E. coli DH5α* strain. We used kanamycin and spectinomycin resistance gene to replace *cueO* and *cusCFBA* genes on the chromosome. Thus we obtained double knockout strain *E. coli DH5α::ΔcueOΔcusCFBA*. After that, we transferred pCWCu1, pCWCu18 and pCWCu44 into *DH5α::ΔcueOΔcusCFBA* strain respectively to obtain Cu8 (*DH5α::ΔcueOΔcusCFBA*/pCWCu1), Cu26 (*DH5α::ΔcueOΔcusCFBA*/pCWCu18) and Cu47 (*DH5α::ΔcueOΔcusCFBA*/pCWCu44) strains by electrical transformation. Finally, pLC8 and pLC17 transferred into Cu1 and Cu8 strains also by electrical transformation to obtain Cu27 (*DH5α*/pCWCu1/pLC8), Cu28 (*DH5α::ΔcueOΔcusCFBA*/pCWCu1/pLC8) and Cu33 (*DH5α*/pCWCu1/pLC17) strains, separately.

Statistics and reproducibility

The statistical analyses performed on the data presented in each figure are detailed in the corresponding figure captions. All analyses were executed using Origin and FlowJo 10.8.1 software. The experiments were conducted with three independent replicates.

Reporting summary

Further information on research design is available in the Nature Portfolio Reporting Summary linked to this article.

Data availability

The data supporting this study's findings are available within the paper and its Supplementary Information files. Should any raw data files be needed in another format, they can be obtained from the corresponding author upon reasonable request. Source data used to generate Figs. 1–6 can be found in Supplementary Data1-3.

Received: 7 May 2024; Accepted: 21 October 2024;
Published online: 29 October 2024

References

1. Liu, Y. et al. Rapid and selective detection of trace Cu^{2+} by accumulation- reaction-based Raman spectroscopy. *Sens. Actuators B Chem.* **283**, 278–283 (2019).
2. Yang, Y. et al. Exploring cuproptosis as a mechanism and potential intervention target in cardiovascular diseases. *Front. Pharmacol.* **14**, 1229297–1229297 (2023).
3. Willianne, I. V., Cisca, W. & Bart, S. D. V. Relevance of animal models for understanding mammalian copper homeostasis. *Am. J. Clin. Nutr.* **88**, 840S–845SS (2008).
4. Eija, P. et al. Excess copper predisposes photosystem II to photoinhibition in vivo by outcompeting iron and causing decrease in leaf chlorophyll. *Plant Physiol.* **129**, 1359–1367 (2002).
5. Maksymiec, W. Effect of copper on cellular processes in higher plants. *Photosynthetica* **34**, 321–342 (1998).
6. Samprit, B., Sourav, M. & Angana, S. Review of microbial biosensor for the detection of mercury in water. *Environ. Qual. Manag.* **31**, 29–40 (2021).
7. Michael, M. et al. Microbial whole-cell biosensors: current applications, challenges, and future perspectives. *Biosens. Bioelectron.* **191**, 113359 (2021).
8. Changjiang, L. et al. Engineering whole-cell microbial biosensors: design principles and applications in monitoring and treatment of heavy metals and organic pollutants. *Biotechnol. Adv.* **60**, 108019–108019 (2022).
9. Zengling, M. et al. Recent advances in the analytical strategies of microbial biosensor for detection of pollutants. *Chemosphere* **306**, 135515–135515 (2022).
10. Dong, S. & Zhai, J. Biosensors: microbial sensors. *Ref. Modul. Biomed. Sci.* **1**, 405–419 (2023).
11. Tess, L. B., Gülay, M. & Edwin, A. F. Environmental sensing of heavy metals through whole cell microbial biosensors: a synthetic biology approach. *ACS Synth. Biol.* **4**, 535–546 (2015).
12. Karrera, Y. D. et al. Interplay between tolerance mechanisms to copper and acid stress in Escherichia coli. *Proc. Natl Acad. Sci. USA* **114**, 6818–6823 (2017).
13. Yilin, P. et al. Development of a sensitive *Escherichia coli* bioreporter without antibiotic markers for detecting bioavailable copper in water environments. *Front. Microbiol.* **10**, 3031 (2019).
14. Rensing, C. & Grass, G. Escherichia coli mechanisms of copper homeostasis in a changing environment. *FEMS Microbiol. Rev.* **27**, 197–213 (2003).
15. Outten, F. W., Huffman, D. L., Hale, J. A. & O'Halloran, T. V. The independent cue and cus systems confer copper tolerance during aerobic and anaerobic growth in Escherichia coli. *J. Biol. Chem.* **276**, 30670–30677 (2001).
16. Kinga, B. & Zofia, P. Molecular basis of active copper resistance mechanisms in Gram-negative bacteria. *Cell Biol. Toxicol.* **29**, 397–405 (2013).
17. Fu, B. et al. Metal-induced sensor mobilization turns on affinity to activate regulator for metal detoxification in live bacteria. *Proc. Natl Acad. Sci. USA* **117**, 13248–13255 (2020).
18. He, R. et al. Copper stress by nutritional immunity activates the CusS-CusR two-component system that contributes to Vibrio alginolyticus anti-host response but affects virulence-related properties. *Aquaculture* **532**, 736012 (2021).
19. Delmar, J. A., Su, C. C. & Yu, E. W. Heavy metal transport by the CusCFBA efflux system. *Protein Sci.* **24**, 1720–1736 (2015).
20. Yerin, K. et al. Enhancing the copper-sensing capability of Escherichia coli-based whole-cell bioreporters by genetic engineering. *Appl. Microbiol. Biotechnol.* **102**, 1513–1521 (2018).

21. Ravikumar, S. et al. Construction of a bacterial biosensor for zinc and copper and its application to the development of multifunctional heavy metal adsorption bacteria. *Process Biochem.* **47**, 758–765 (2012).
22. Sambandam, R. et al. Modification of CusSR bacterial two-component systems by the introduction of an inducible positive feedback loop. *J. Ind. Microbiol. Biotechnol.* **39**, 861–868 (2012).
23. Hsuan, P. C. et al. Development of a pigment-based whole-cell biosensor for the analysis of environmental copper. *RSC Adv.* **7**, 29302–29305 (2017).
24. Wang, B., Barahona, M. & Buck, M. A modular cell-based biosensor using engineered genetic logic circuits to detect and integrate multiple environmental signals. *Biosens. Bioelectron.* **40**, 368–376 (2013).
25. Taniguchi, Y. et al. Quantifying *E. coli* proteome and transcriptome with single-molecule sensitivity in single cells. *Science* **329**, 533–538 (2010).
26. Jiajia, L. et al. A self-amplifying plasmid based ultrasensitive biosensor for the detection of As(III) in water. *Biosens. Bioelectron.* **221**, 114937–114937 (2023).
27. Novoa-Aponte, L., Xu, C., Soncini, F. C. & Argüello, J. M. The two-component system CopRS maintains subfemtomolar levels of free copper in the periplasm of pseudomonas aeruginosa using a phosphatase-based mechanism. *mSphere* **5**, e01193–20 (2020).
28. Siryaporn, A. & Goulian, M. Cross-talk suppression between the CpxA-CpxR and EnvZ-OmpR two-component systems in E. coli. *Mol. Microbiol* **70**, 494–506 (2008).
29. Olga, V. S. et al. New findings on GFP-like protein application as fluorescent tags: Fibrillogenesis, oligomerization, and amorphous aggregation. *Int. J. Biol. Macromol.* **192**, 1304–1310 (2021).
30. Ping, L. et al. PcoB is a defense outer membrane protein that facilitates cellular uptake of copper. *Protein Sci.* **31**, e4364–e4364 (2022).
31. Wu, W. et al. Biodetection and bioremediation of copper ions in environmental water samples using a temperature-controlled, dual-functional *Escherichia coli* cell. *Appl. Microbiol. Biotechnol.* **103**, 6797–6807 (2019).
32. Affandi, T., Issaian, A. V. & McEvoy, M. M. The structure of the periplasmic sensor domain of the Histidine Kinase CusS shows unusual metal ion coordination at the dimeric interface. *Biochemistry* **55**, 5296–5306 (2016).
33. Hiroyuki, U. et al. Cooperative regulation of the common target genes between H_2O_2-sensing YedVW and Cu^{2+}-sensing CusSR in Escherichia coli. *Microbiology* **161**, 729–738 (2015).

Acknowledgements

X.F., Y.F., and J.L. were supported by the National Natural Science Foundation of China (no. 32171245) and Fundamental Research Funds for the Central Universities (no. 2412022QD011). X.F. and J.L. acknowledge the support from the Jilin Provincial Department of Education (China), the Key Laboratory of Nanobiosensing and Nanobioanalysis at Universities of Jilin Province (China), and the Analysis and Testing Center of Northeast Normal University (China).

Author contributions

X.F. designed and supervised the projects. Y.F. engineered the strains, performed the all the experiments and data analysis. J.L. constructed some of original plasmids. X.F. and Y.F. wrote the manuscript with comments from all authors. X.F., E.W., and J.W. discussed and interpreted the results, reviewed and edited the manuscript.

Competing interests

The authors declare no competing interests.

Additional information

Supplementary information The online version contains supplementary material available at https://doi.org/10.1038/s42003-024-07112-6.

Correspondence and requests for materials should be addressed to Xiaona Fang.

Peer review information *Communications Biology* thanks Prasanta Kumar Hota, Jun Kurushima and the other, anonymous, reviewer(s) for their contribution to the peer review of this work. Primary Handling Editor: Ophelia Bu.